Impact of gold nanoparticles combined to X-Ray irradiation on bacteria

A. Simon-Deckers[1], E. Brun[2], B. Gouget[1], M. Carrière[1], C. Sicard-Roselli[2]

[1] Laboratoire Pierre Süe, UMR9956 CEA-CNRS, Gif sur Yvette, France
[2] Laboratoire de Chimie Physique, UMR 8000 CNRS-Université Paris 11, Orsay, France

Abbreviations:

CTAB: Cetyl Trimethyl Ammonium Bromide
DMEM: Dulbecco's Modified Essential Medium
GNP: Gold nanoparticle
LB: Luria Bertani
MTT: 3-(4,5-dimethylthiazol-z-yl)-2,5-dipheny-tetrazotium bromide
NIR: Near-Infrared
NP: Nanoparticle
PEG: Polyethylene glycol
TEM: Transmission Electron Microscopy

Abstract

Recent increase of multi drug-resistant bacteria represents a crucial issue of public health. As novative approaches are required to face that problem, those emerging from nanotechnology are of great interest. In that context we propose the possibility to use gold nanoparticles combined with ionising radiation to destroy pathogenic bacteria. For that, we investigated the potential X-Rays enhanced reduction of bacterial cell viability, following nanoparticle exposure, on a bacterial model, _Escherichia coli_. Our first concern was to confirm the absence of toxicity of the colloidal solution used. Then, we developed an X-Ray irradiation system and showed that gold nanoparticles increased the efficiency of ionising radiation to induce bacteria cell death.

Introduction

Since the last decade, nanomaterials showed an exponential progression in domains such as chemistry and biology. Thus, development of nanotechnologies may lead to an increasing nanomaterials release in the environment and so potential risks for ecosystems. Few studies deal with the impact of nanoparticles on the ecosystem [1, 2]. Most of them concern aquatic animals [3] and bacteria. Two concerns are important in case of bacterial contamination with nanomaterials: if nanomaterials are toxic for environmental bacteria, they can have devastating effects on the ecosystems and lead to a global destabilization. On the opposite, if bacteria are resistant to nanomaterials, adsorb them onto their membrane or absorb them in their periplasm or cytoplasm, they can be responsible for their transfer in the environment. This mobilization can thus lead to the transfer of nanoparticles from the site of contamination to non-contaminated areas. Some nanoparticles (NPs), such as silver NPs, have been shown to have antibacterial properties [4, 5]. Their mode of action was proposed to be identical to the one of Ag ions, _i.e._ the positively charged Ag NPs interact strongly with the cell membrane modifying its permeability. For this reason they are used for industrial purposes, for example as adjuvant in textiles [6, 7] or in bone cement [8, 9]. They are described to be able to inhibit the proliferation of pathogens [10], and thus have interesting medicinal applications. If this toxicity is beneficial for such applications, it suggests ecotoxicological issues in case of dissemination in the environment, which makes it difficult to consider them as potentially usable for other technological developments. On the opposite and due to their interesting properties, gold nanoparticles (GNPs) have been considered for several potential biological applications going from drug delivery [11, 12] and imaging [13] to therapy [14, 15]. Concerning cancer therapies the most studied effect is known as the photothermal effect: spherical NPs but also nanorods when submitted to a laser beam emit heat enough to kills cells [16]. Another application of GNPs was presented as a radio-sensitizing effect when gold is submitted to an X-Ray beam [17, 18]. All these promising applications would necessitate GNPs vectorisation to target specifically cancer cells and to avoid high dose GNPs injections. Nevertheless, human exposure to nanoparticles requires nanotoxicologic research to ensure the absence of toxicity of the particles but also of the targeting coating. Cytotoxicity of NPs is an emerging field of research [19-22] and their impact on human cell lines was recently reviewed by Lewinski _et al_ [23]. The variety of tests, cell types and nanoparticles (coating, concentration and incubation time) make difficult an accurate comparison. Nevertheless a general trend can be drawn _i.e._ GNPs do not induce high cell mortality.

Curiously, only few studies deal with impact of GNPs on microbial cells [24, 25]. Williams _et al_ did not note significant decrease in bacterial growth of _Escherichia coli_ (_E. coli_) exposed to up to $1.1 \ 10^{-4} \ g \ mL^{-1}$ PEG-coated GNPs whereas Huang and Zharov teams combined GNPs and near infra-red (NIR) light or laser pulses to potentially use GNPs

for antimicrobial activities. As for us, we got interested in the destruction of bacteria using GNPs and ionising radiation and precisely on the possible radio-enhancement effect of GNPs. Our first goal was to check the absence of toxicity of GNPs on *E. coli* under our conditions and then to determine the ability of GNPs to enhance X-Ray-induced degradation. For that we designed an X-Ray system devoted to biological samples irradiation.

Materials and methods

Nanoparticles synthesis and characterization

Non-functionalized gold nanoparticles synthesis
All glassware used for GNPs synthesis was thoroughly washed with aqua regia (3:1 HNO_3, HCl), rinsed extensively with water and oven-dried at 60°C. The colloidal gold nanoparticles were prepared by the Turkevitch method [26, 27], *i.e.* citrate thermal reduction. Typically, 4.2 mL of a 1% (w/v) solution of tri-sodium citrate were added to 100 mL of a 10^{-3} mol. L^{-1} $KAuCl_4$ aqueous solution. The mixture was heated under moderate stirring until 10 minutes after the solution had turned purple. It was then subjected to centrifugation (2300 g, 20 min) and the pellet of NPs was collected. The final concentration was 6 mg/mL of gold.

Electron microscopy
Transmission electron microscopy (TEM) was used to obtain images of the NPs. A drop of stock solution of GNPs suspension was placed on carbon-coated copper grids (300 mesh) and dried before being placed in the TEM for imaging. NPs diameter distribution was determined with ImageJ software [28] by analyzing more than 400 particles.

Characterization of the interaction of GNPs with bacteria was done after exposure to 50 µg.mL^{-1} for 24 h. For that, bacterial pellets were fixed with 2.5% glutaraldehyde, post-fixed with OsO_4 and dehydrated in graded concentrations of ethanol, then embedded in Epon resin. 80 nm thin sections were cut, and observed with a CM 120 Philips electron microscope at 80 kV at the CCME (Centre Commun de Microscopie Electronique d'Orsay).

Cell culture

NRK-52E cell line is a model for rat kidney proximal tubules and Hep-G2 hepatocarcinoma cell line are classically used for human liver toxicity assessment. NRK-52E were purchased from ATCC (CRL-1571), and Hep-G2 kindly given by Dr. D. Cassio (INSERM U442). These cell models were chosen since in case of contamination and of translocation of GNPs in the bloodstream, liver and kidneys, as detoxification organs, are the more probable targets of GNPs toxicity. They were grown in DMEM supplemented with 10% (V/V) foetal bovine serum, 2 mM L-glutamine, 50 UI/mL penicillin and 50 µg/mL streptomycin. They were maintained at 37°C in a 5% CO_2 incubator and passed at 80% of confluence. Exposures to nanomaterials were done on sub-confluent cells.

Toxicity assays

Cells were seeded in 96-well plates and exposed after 24 h to 100 µL of GNPs in the presence or absence of citrate (0-200 µg/mL) in cell culture medium without serum to avoid interaction with nanoparticles (see figure legends for details). Cell metabolic activity, reflecting cytotoxicity, was assessed by using 3-(4,5-dimethylthiazol-z-yl)-2,5-dipheny-tetrazotium bromide (MTT) [29]. Mitochondrial dehydrogenases of viable cells reduce MTT to water-insoluble blue formazan crystals; this assay thus indicates cell mitochondrial activity impairment. After exposure, 10 µL of a 5 mg/mL MTT solution were added to each well. After 1 h at 37°C, medium was then replaced by 100 µL of dimethyl sulfoxide and mixed thoroughly to dissolve the formazan crystals. Nanoparticles were allowed to sediment during 1 h and 50 µL of each well was then transferred to another plate. Absorbance was measured at 570 nm with a Gemini X spectrophotometer (Molecular Devices, St Grégoire, France).

Bacterial strain and growth conditions

E. coli K-12 MG1655 bacteria (CGSC 7740) [30] were grown aerobically at 37°C in Luria Bertani broth (LB) medium under 200 rpm agitation. This strain was chosen since it approximates wild-type *E. coli*, because it was subjected to minimal genetic manipulations. For GNPs exposure, a preculture was obtained by growing cells until mid-exponential phase. Since GNPs immediately aggregate when the suspension is diluted in LB medium due to its high ionic strength, cells were washed and exposed to GNPs in sterile ultrapure water. Equivalent volumes of bacteria (DO = 6 at 600 nm) and of GNPs were incubated prior to irradiation. Control cultures were grown under identical conditions in the absence of GNPs. Exposures were conducted with a constant 300 rpm shaking for 24 h.

Live/Dead toxicity assay

Following GNPs exposure, the bacteria were stained using the Live/Dead BacLight Bacterial Viability Kit (Invitrogen) following the manufacturer's instruction. This assay uses two dye components, the green-fluorescent SYTO® 9 stain and the red-fluorescent propidium iodide stain. These stains differ in their ability to penetrate healthy bacterial cells: SYTO 9 stain labels both live and dead bacteria while propidium iodide penetrates only bacteria with damaged membranes. Thus, live bacteria with intact membranes fluoresce green, while dead bacteria with damaged membranes fluoresce red. Live and dead bacteria can be quantified separately by fluorescence microscopy (excitation at 470 nm; emission at 525 and 625 nm; Gemini X spectrophotometer, Molecular Devices, St Grégoire, France). Percentage of cell viability was calculated after bacteria exposure to GNPs compared to control.

Irradiations and dosimetry

A new X-Ray irradiation system was designed and adapted for biological samples. This system is based on a crystallographic generator with a ceramic diffraction tube. The originality of
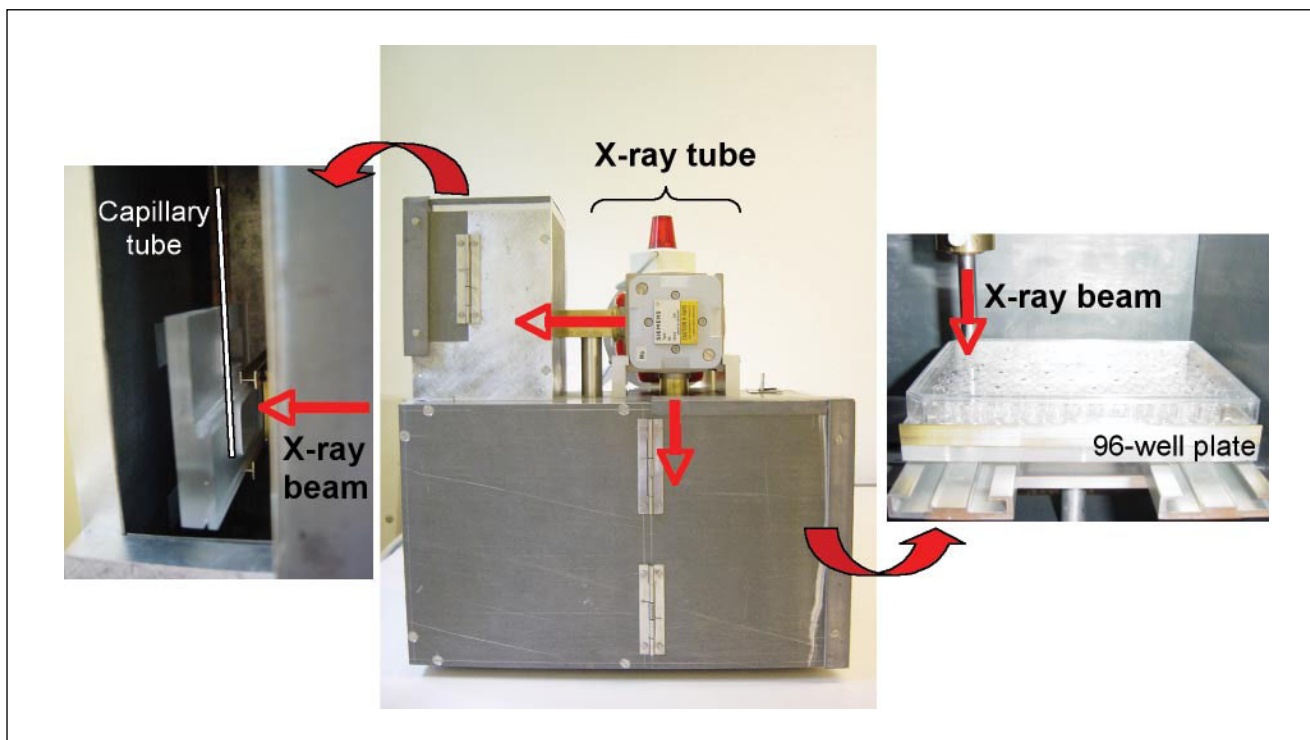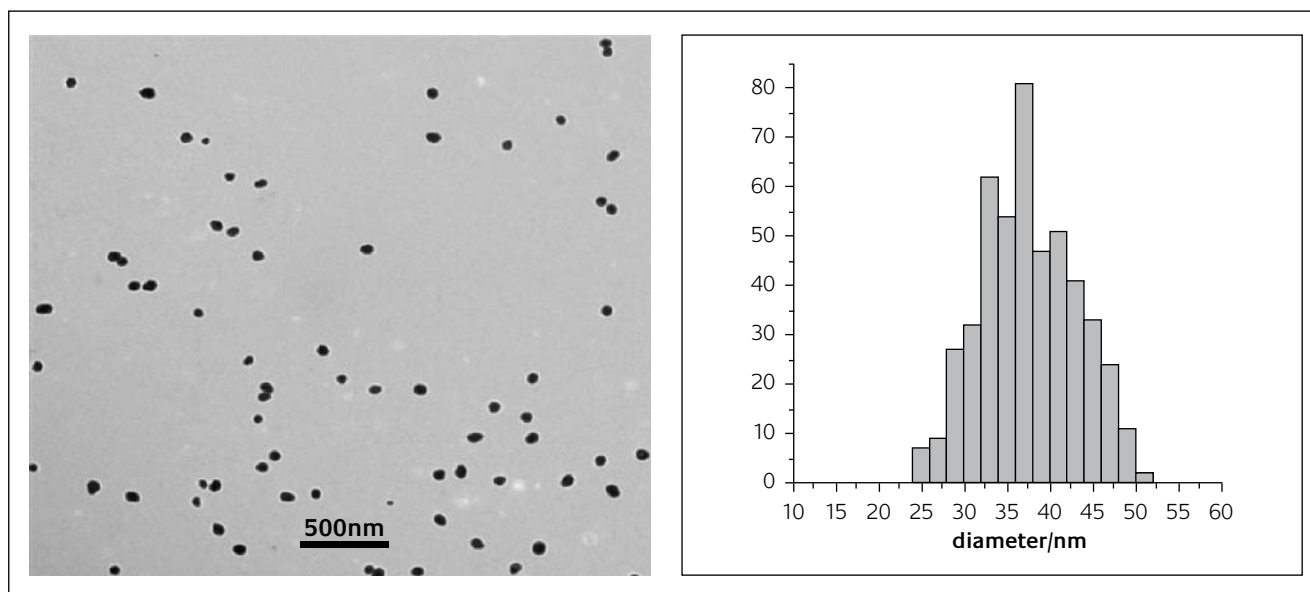
Figure 1

Pictures of the X-ray irradiation system. The X-ray beam is guided along two perpendicular directions. Two cages allow respectively experiments with samples in capillary tubes (left part) and with cell samples in 96-well plates (right part)

this apparatus resides in its two perpendicular windows (Figure 1). In the first one, the horizontal beam allows the irradiation of samples in Lindemann capillary tubes (Glas Tecnik&Konstruktion, Germany) or plastic cuvettes. Several tubes can be irradiated at the same time. The second beam is vertical and equipped with a sample holder designed to irradiate cells contained in 96-well plates. Temperature regulation of the plate is under realisation. These two beams can be used simultaneously and independently. In addition, dose rate can be easily tuned, playing with the generator power and the sample distance from

the source. In the present case, irradiations were performed in plastic cuvettes with a copper anti-cathod (Diffractis 601 Enraf Nonius X-ray generator, 40 kV, 20 mA). The predominent photon energy was about 8 keV.

As the irradiation system was new, an accurate dosimetry was necessary. A usual dosimeter for high-energy photons is the chemical Fricke dosimeter. Under irradiation, Fe(II) ions in an acidic solution are converted into Fe(III). This oxidation yield is known with high precision for gamma radiation and hard X-rays. But for X-rays with energies between 1.5-10 keV,

Figure 2

Transmission electron microscopy images of gold nanoparticles (LEFT) and size distribution (RIGHT)
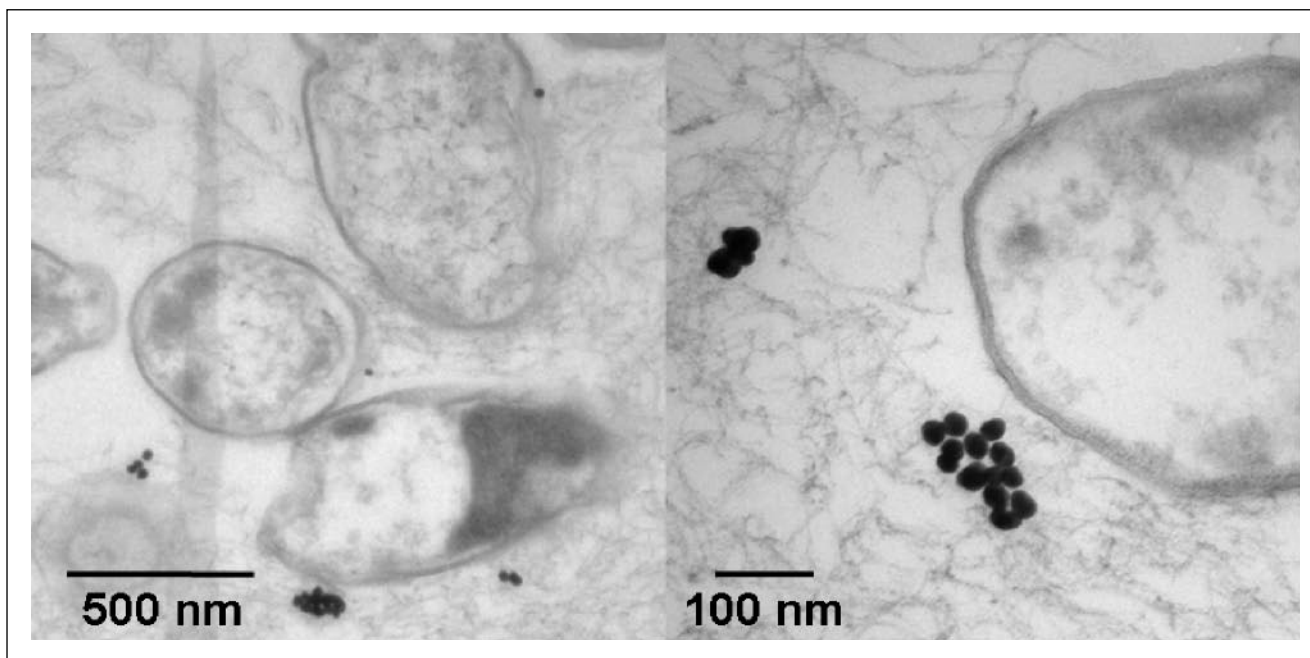
Figure 3

Transmission electron microscopy observation of E. coli exposed to gold nanoparticles. Bacteria were cultivated in LB medium, then rinsed and exposed to GNPs in water during 24 h. After embedding in Epon, thin sections were cut and directly observed

available values of $G(Fe^{3+})$ are more controversial [31]. So we turned to a radiochromatic dosimetry for the newly−developed X-rays generator. Dose rate measurement using Gafchromic® HD-810 radiochromatic dosimetry film (ISP Technologies INC, Wayne, NJ) are described thoroughly elsewhere [32]. Briefly, this film has a nominal 7-μm-thick radiation sensitive layer on a 100 μm polyester base. Film samples were placed in plastic cuvettes and exposed to X-rays for various durations. After storage in the dark for 48h, they were scanned with a CanoScan LIDE 500F scanner and blue channel images were analysed with ImageJ software [28]. The absorbance was defined as $\log_{10}(I_0/I)$ where I_0 and I are the mean values resulting from the ImageJ histograms for respectively non-exposed and exposed zones of the samples. The conversion from absorbance to absorbed dose in water resulted from previous work [33]. For all experiments, the equivalent dose rate in water obtained was 10.7 Gy/min. Bacteria were always kept at 37°C except for irradiation that was done at room temperature under normal atmosphere.

Results and discussion

Gold nanoparticles / bacterial cells interaction and toxicity

Gold nanoparticles were synthesized using the well-known method of citrate reduction. The spherical particles obtained were characterized using transmission electron microscopy. Their size distribution was determined by analysing more than 400 objects. Figure 2 shows that the average size is 37.5 ± 5.6 nm. The concentration of citrate versus gold salts is known to govern the size and shape of the colloids obtained [34]. In our case, we used an excess of citrate to obtain this

size of nanoparticles. Therefore, citrate is still present at the surface of the GNPs, and plays then a double role: reducing agent and stabilizer. Bacteria NPs interaction was investigated using electron microscopy. As already mentioned by Huang *et al.* [35], non-modified GNPs show no specific interaction with the cell walls of the bacteria (Figure 3), due to repulsive forces caused by negative surface charges of bacteria and nanoparticles. In our conditions, GNPs were observed either isolated at the vicinity of bacteria, or grouped in small clusters of 5-15 NPs. No specific modification of bacteria morphology was observed: they presented large intracellular vacuoles but so did control bacteria. These vacuoles certainly come from the stress generated by exposure in water. However these vacuoles did not inhibit bacterial growth when they were re-seeded in LB medium, *i.e.* this stress was reversible. Nanoparticles sometimes went close to bacteria, were rarely adsorbed on bacterial surface, but we never observed nanoparticles in bacterial periplasm or cytoplasm.

Toxicity of GNPs was investigated on this bacterial strain. We have chosen not to functionalize nanoparticles in order to get rid of functionalizing molecule self toxicity, which would introduce artefacts in the study. Effectively Connor *et al* showed that CTAB [21] used as a stabilizer of the nanoparticles induces cell toxicity. Since our synthesis procedure induces contamination of nanoparticle suspension with citrate, the first control consisted in bacteria exposed to citrate only. To do so, nanoparticles were centrifuged and the supernatant was collected. The absence of nanoparticles in the supernatant was verified by UV-Visible absorption (not shown). 40 μL of a bacteria solution (DO = 3.5) was incubated with 50 μL of nanoparticle suspension supernatant, or with 50 μL of water, or 50 μL of gold nanoparticles to quantify their respective toxicities. Figure 4 shows that the three samples exhibit the
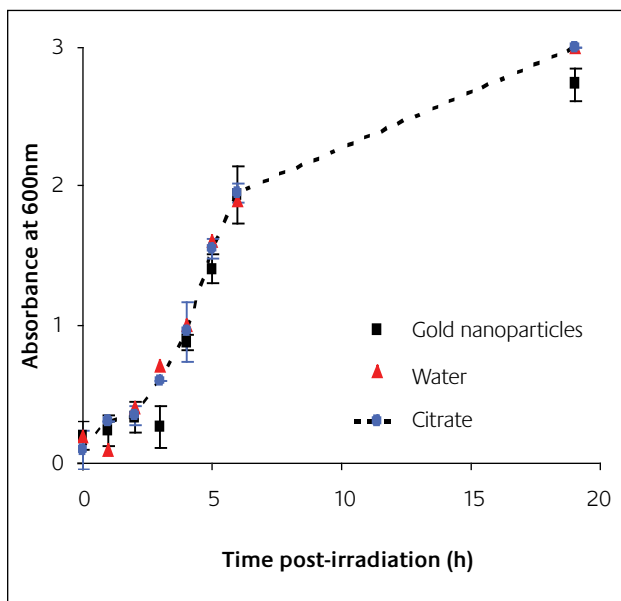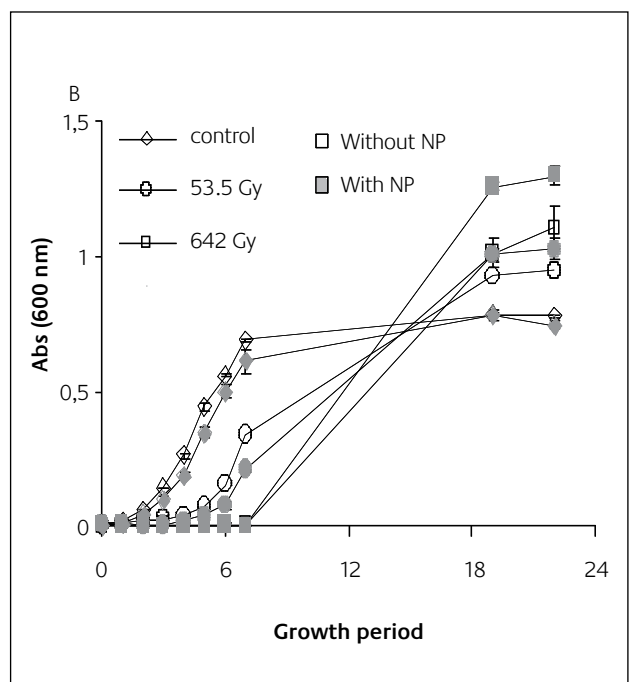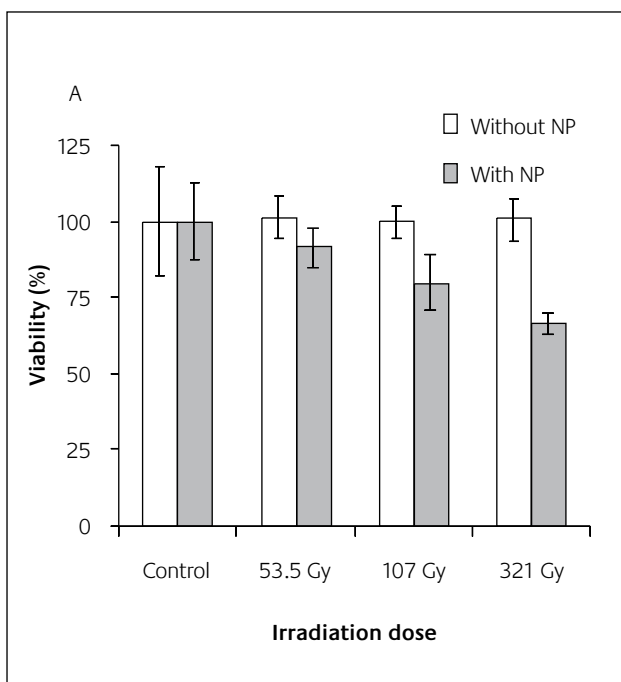
Figure 4

Growth curve of E. coli. Bacteria were rinsed and exposed 24 h in water either to GNP synthesized in citrate, or to an aqueous citrate solution. They were then seeded in LB medium and allowed to grow

same behaviour *i.e.* the bacteria possess the same lag phase and the same growing profile in the presence of water or citrate, and also in the presence of gold nanoparticles. We can then conclude from that experiment that GNPs synthesized in the presence of citrate do not induce any toxicity on *E. coli* even at high concentration of GNPs (3mg/mL final). In their article, Huang *et al* did not discuss GNPs toxicity to bacterial strains, they rather focused on GNPs plus NIR photothermal

treatment effect on several bacterial strains [35]. From their results, it seems that non-functionalized GNPs are not toxic to *E. coli* DH5α bacteria, but GNPs functionalized with vancomycin (GNP@van) are toxic. Moreover GNPs did not adsorb onto bacterial membranes while GNP@van did. Our results thus confirm these data, since the GNPs we used were not toxic and did not adsorb onto bacterial membrane.

To consider GNPs as potentially radio-sensitizing, it is essential to validate that they are not toxic to human cells. We performed toxicity experiments on NRK-52E and Hep-G2 cells, models for liver and kidneys which would be the most probably exposed organs if GNPs reach the bloodstream in case of a contamination. Indeed, in rats, 50 nm-diameter GNPs injected intravenously were shown to accumulate preferentially in liver and spleen [22]. NRK-52E and Hep-G2 cells were exposed to 0-200 μg/mL GNPs during 24 h. We found gold nanoparticles as non cytotoxic, as only 0 to 10% of cell death was measured on both cell lines using MTT assay (not shown). In fact, up to now, few studies describe citrate/GNPs toxicity on human cells [21, 36, 37]. Connor *et al* found citrate/GNPs of 18 nm non-toxic up to 250 μM (gold atoms) on K562 Leukaemia cells. Conversely, when higher concentration of GNPs were used by Pernodet *et al*, it could be evidenced a toxicity of citrate/GNP (0.1 and 0.6 mg/ml) on human dermal fibroblasts showing a dose-dependent decrease in cell density and area. The difference between this result and ours can come from the size of GNPs, which have a 20 nm-diameter in the study of Pernodet, and around 40 nm in our study. Moreover cell type can be an explanation and dermal fibroblasts might then be more sensitive to GNPs than NRK-52E and HepG2 cells.

Figure 5

Impact of irradiation on E. coli pre-exposed to gold nanoparticles or not. Viability of E. coli after 0, 53.5, 107, 321 or 642 Gy of irradiation, after exposure to gold nanoparticles (grey) or not (white). Global viability was assessed with the live/dead assay (A) or growth curves construction after re-seeding in LB medium (B)

Radio-sensitizing effect of gold nanoparticles

Nanoparticles possess many potential therapeutical applications. For example, many theoretical as applied studies deal with their photothermic capacity *i.e.* their property to induce an increase in temperature sufficient to kill cells. For example, El-Sayed *et al* showed that the presence of gold nanorods reduces by a factor of 2 the laser power necessary to kill cancer cells [16]. Recently, nanoparticles were applied as photothermal agents for selective-killing of pathogenic bacteria [25, 38]. Non-functionalized gold nanoparticles could induce the destruction of pathogenic bacteria after a near-infrared illumination [35]. This phenomenon is enhanced when nanoparticles are selectively anchored onto the cell walls, using vancomycin or antibodies-coating.

Besides, Herold *et al* [18] and more recently Hainfeld *et al* [17] showed that gold nanoparticles could be used as a radio-sensitizing agent for radiotherapy. The first experiments conducted showed that nanoparticles, resuspended in cell culture or in tumour tissues, and submitted to X-ray radiation induce a higher degradation of malign cells or tumours than radiation alone. This radio-sensitizing effect was also reported *in vitro* for DNA [39, 40] and proteins [33]. In this work, we investigated the capacity of non-functionalized spherical-shaped gold nanoparticles to induce bacterial cell death after X-ray irradiation. The nanoparticles we used had approximately the same size as those used by Huang *et al* [35], *i.e.* 30-40 nm diameter. Ionising radiation is well-known to induce cell death which is quantified using the D value. This value, expressed in kiloGrays (kGy), represents the radiation dose required to reduce by a 1-$\log_{10}$ factor the viability of cells. D is known to vary with the different types of cells and irradiation conditions. In our case, the doses used here are one order of magnitude lower than those necessary to abrogate viability [41]. Figure 5A shows the influence of nanoparticles exposure on bacterial viability after 0, 53.5, 107 or 321 Gy of X-ray irradiation. Nanoparticle-exposed bacterial cells viability was normalized to non-exposed bacterial cell viability. A global tendency to enhanced bacterial death is observed, decreased viability was significant after 321 Gy. This result shows that GNPs have a radio-sensitizing effect on bacteria. When these GNP- and X-ray exposed bacteria were then reseeded in culture medium and allowed to grow, it was observed that X-ray irradiation induced a dose-dependent decrease in bacterial viability, demonstrated by an increased lag-phase (5B). However when comparing growth curves, irradiated bacteria were still able to proliferate, and the growth curve had the same appearance (Figure 5B). Lag phases and growth speed were statistically similar. It might be that irradiation caused the death of some bacteria but not all, and that viable bacteria proliferated as non-irradiated bacteria.

Cell-killing properties of vancomycin-coated, 30 nm-diameter gold nanoparticles combined to near-infrared irradiation have been demonstrated on pathogenic bacteria - [35]. In this previous work, gold nanoparticles were polygonal-shaped, and their selective-killing activity was related to photothermal properties, due to their capacity to absorb NIR light, leading to hyperthermia. After 5-min of NIR irradiation in the presence of nanoparticles, the temperature increases to lethal temperature for the bacteria, estimated to be at least 50°C, resulting in bacteria killing. This cell death was further amplified by the presence of functionalized gold nanoparticles. Our report suggests that even non-functionalized gold nanoparticles, which do not adhere on bacterial cell wall, have bacterial killing properties when combined to X-Ray radiation. The difference of bacterial cell killing efficiency of the nanoparticles we used compared to those used by Huang *et al* [35] can be attributed to the kind of irradiation *i.e.* the photon energy. It is highly probable that the mechanisms involved are different. Contrary to NIR light, X-ray radiation has not been shown to induce significant temperature elevation, though the mechanism is still unclear. Most probably direct or indirect damages are generated, respectively DNA strand breaks and generation of free radicals from the ionization of water molecules.

Conclusion

We have generated gold nanoparticles which are not toxic to bacterial cells, and which did not accumulate in bacteria. These nanoparticles are ecotoxically safe, and will not be mobilized by bacteria, *i.e.* transferred in the ecosystems, leading to their dissemination. We also adapted an X-ray irradiation system, especially designed for biological samples. Combined to X-ray irradiation, pre-exposure of bacteria to these nanoparticles led to a tendency of radio-sensitization of bacteria, but this tendency was not statistically significant. Future work will focus on nanoparticles functionalization, in order to induce specific adsorption of nanoparticles on bacterial cell walls, which could enhance the radio-sensitizing effect. However special care should be taken when using functionalization as such nanoparticles could be less safe than those we used in the present study.

Gold nanoparticles submitted to X-ray radiation appear to be a potential tool for anti-microbial proliferation system or pathogenic bacteria killing system. For example, they could be used as antibacterial gold nanocomposite coatings on materials, decontaminated by the application of X-ray radiation. The emergence of resistant bacteria to traditional antibiotics motivates such a development of new antibacterial systems.

About the authors

Angélique Simon-Deckers is a PhD student working at the Pierre Süe Laboratory, CEA-CNRS UMR 9956, Saclay, France. Her research focuses on biological effects of nanomaterials on *in vitro* cultured cells and on bacteria.

Emilie Brun is a PhD student working at the Laboratoire de Chimie Physique, Université Paris XI Orsay, CNRS UMR 8000, Orsay, France. Her research interest includes gold nanoparticle radio-sensitizing effect.

Dr. Barbara Gouget was permanent researcher at the Pierre Süe Laboratory, CEA-CNRS UMR 9956, Saclay, France when these experiments were done. She is now working at the Scientific Department of the French Food Safety Agency, Maisons-Alfort, France.

Dr. Marie Carrière is permanent researcher at the Pierre Süe Laboratory, CEA-CNRS UMR 9956, Saclay, France. Her area of research includes human and ecotoxicity of environmental pollutants *i.e.* metals, radionuclides, and nanomaterials. Models employed are *in vitro* cultured cells, bacteria and plants cultivated in hydroponic solutions.

Dr. Cécile Sicard-Roselli is an Associate Professor in the Laboratoire de Chimie Physique, Université Paris XI Orsay, CNRS UMR 8000, Orsay, France. Her area of research includes radiobiology, analytical chemistry and nanosciences (gold nanoparticles).

References

1   V.L. Colvin, *Nat. Biotechnol.*, 2003, **21**, 1166

2   B. Nowak, T.D. Bucheli, *Environ. Poll.*, 2007, **150**, 5

3   M.N. Moore, *Environ. Int.*, 2006, **32**, 967

4   J.S. Kim, E. Kuk, K.N. Yu, J.H. Kim, S.J. Park, H.J. Lee, S.H. Kim, Y.K. Park, Y.H. Park, C.Y. Hwang, Y.K. Kim, Y.S. Lee, D.H. Jeong, M.H. Cho, *Nanomedicine*, 2007, **3**, 95

5   C.N. Lok, C.M. Ho, R. Chen, Q.Y. He, W.Y. Yu, H. Sun, P.K. Tam, J.F. Chiu, C.M. Che, *J. Biol. Inorg. Chem.*, 2007, **12**, 527

6   T. Yuranova, A.G. Rincon, C. Pulgarin, D. Laub, N. Xantopoulos, H.-J. Mathieu, J. Kiwi, *J. Photochem. Photobiol. A: Chemistry*, 2006, **181**, 363

7   T. Yuranova, A.G. Rincon, A. Bozzi, S. Parra, C. Pulgarin, P. Albers, J. Kiwi, *J. Photochem. Photobiol. A: Chemistry*, 2003, **161**, 27

8   Z. Shi, K.G. Neoh, E.T. Kang, W. Wang, *Biomaterials*, 2006, **27**, 2440

9   V. Alt, T. Bechert, P. Steinrucke, M. Wagener, P. Seidel, E. Dingeldein, E. Domann, R. Schnettler, *Biomaterials*, 2004, **25**, 4383

10   N. Tsao, P.P. Kanakamma, T.Y. Luh, C.K. Chou, H.Y. Lei, *Antimicrob. Agents Chemother.*, 1999, **43**, 2273

11   G. Han, P. Ghosh, V.M. Rotello, *Adv. Exp. Med. Biol.*, 2007, **620**, 48

12   G.F. Paciotti, L. Myer, D. Weinreich, D. Goia, N. Pavel, R.E. McLaughlin, L. Tamarkin, *Drug Deliv.*, 2004, **11**, 169

13   D. Nagesha, G.S. Laevsky, P. Lampton, R. Banyal, C. Warner, C. DiMarzio, S. Sridhar, *Int. J. Nanomedicine*, 2007, **2**, 813

14   I.H. El-Sayed, X. Huang, M.A. El-Sayed, *Cancer Lett.*, 2006, **239**, 129

15   D. Pissuwan, S.M. Valenzuela, M.B. Cortie, *Trends Biotechnol.*, 2006, **24**, 62

16   X. Huang, I.H. El-Sayed, W. Qian, M.A. El-Sayed, *J. Am. Chem. Soc.*, 2006, **128**, 2115

17   J.F. Hainfeld, D.N. Slatkin, H.M. Smilowitz, *Phys. Med. Biol.*, 2004, **49**, N309

18   D.M. Herold, I.J. Das, C.C. Stobbe, R.V. Iyer, J.D. Chapman, *Int. J. Radiat. Biol.*, 2000, **76**, 1357

19   M. Tsoli, H. Kuhn, W. Brandau, H. Esche, G. Schmid, *Small*, 2005, **1**, 841

20   P. Mukherjee, R. Bhattacharya, N. Bone, Y.K. Lee, C.R. Patra, S. Wang, L. Lu, C. Secreto, P.C. Banerjee, M.J. Yaszemski, N.E. Kay, D. Mukhopadhyay, *J. Nanobiotech.*, 2007, **5**, 4

21   E.E. Connor, J. Mwamuka, A. Gole, C.J. Murphy, M.D. Wyatt, *Small*, 2005, **1**, 325

22   W.H. De Jong, W.I. Hagens, P. Krystek, M.C. Burger, A.J. Sips, R.E. Geertsma, *Biomaterials*, 2008, **29**, 1912

23   N. Lewinski, V. Colvin, R. Drezek, *Small*, 2008, **4**, 26

24   D.N. Williams, S.H. Ehrman, T.R. Pulliam Holoman, *J. Nanobiotech.*, 2006, **4**, 3

25   V.P. Zharov, K.E. Mercer, E.N. Galitovskaya, M.S. Smeltzer, *Biophys. J.*, 2006, **90**, 619

26   J. Turkevitch, *Gold Bull.*, 1985, **18**, 86

27   J. Turkevitch, P.C. Stevenson, J. Hillier, *Faraday Soc.*, 1951, **11**, 55

28   M.D. Abramoff, P.J. Magelhaes, S.J. Ram, *Biophoton. Int.*, 2004, **11**, 36

29   T. Mosmann, *J. Immunol. Methods*, 1983, **65**, 55

30   F.R. Blattner, G. Plunkett, 3rd, C.A. Bloch, N.T. Perna, V. Burland, M. Riley, J. Collado-Vides, J.D. Glasner, C.K. Rode, G.F. Mayhew, J. Gregor, N.W. Davis, H.A. Kirkpatrick, M.A. Goeden, D.J. Rose, B. Mau, Y. Shao, *Science*, 1997, **277**, 1453

31   R. Watanabe, N. Usami, K. Kobayashi, *Int. J. Radiat. Biol.*, 1995, **68**, 113

32   Z. Cai, X. Pan, D. Hunting, P. Cloutier, R. Lemay, L. Sanche, *Phys. Med. Biol.*, 2003, **48**, 4111

33 E. Brun, P. Duchambon, Y. Blouquit, L. Sanche, C. Sicard-Roselli, *Actually submitted*, 2008

34 S. Kumar, K.S. Gandhi, R. Kumar, *Ind. Eng. Chem. Res.*, 2007, **46**, 3128

35 W.C. Huang, P.J. Tsai, Y.C. Chen, *Nanomed*, 2007, **2**, 777

36 X.L. Wei, Z.H. Mo, B. Li, J.M. Wei, *Colloids Surf. B Biointerfaces*, 2007, **59**, 100

37 N. Pernodet, X. Fang, Y. Sun, A. Bakhtina, A. Ramakrishnan, J. Sokolov, A. Ulman, M. Rafailovich, *Small*, 2006, **2**, 766

38 R.S. Norman, J.W. Stone, A. Gole, C.J. Murphy, T.L. Sabo-Attwood, *Nano Lett.*, 2008, **8**, 302

39 E.A. Foley, J.D. Carter, F. Shan, T. Guo, *Chem. Comm. (Camb)*, 2005, 3192

40 Y. Zheng, D.J. Hunting, P. Ayotte, L. Sanche, *Radiat. Res.*, 2008, **169**, 19

41 A. Trampuz, K.E. Piper, J.M. Steckelberg, R. Patel, *J. Med. Microbiol.*, 2006, **55**, 1271